ELSEVIER

Journal of Nuclear Materials 279 (2000) 139–152

journal of nuclear materials

www.elsevier.nl/locate/jnucmat

Tritium profiles in tiles from the first wall of fusion machines and techniques for their detritiation

R.-D. Penzhorn [a,*], N. Bekris [a], W. Hellriegel [a], H.-E. Noppel [a], W. Nägele [b], H. Ziegler [b], R. Rolli [b], H. Werle [c], A. Haigh [d], A. Peacock [d]

[a] *Forschungszentrum Karlsruhe, Technik und Umwelt, Tritium Laboratory, Experimental Engineering Department, P.O. Box 3640, 76021 Karlsruhe, Germany*

[b] *Forschungszentrum Karlsruhe, Technik und Umwelt, Hot Cells, Experimental Engineering Department, P.O. Box 3640, 76021 Karlsruhe, Germany*

[c] *Forschungszentrum Karlsruhe, Technik und Umwelt, Institute for Nuclear and Energy Technology, P.O. Box 3640, 76021 Karlsruhe, Germany*

[d] *JET Joint Undertaking, Abingdon, Oxfordshire OX14 3EA, UK*

Received 1 October 1999; accepted 8 February 2000

Abstract

Tritium profiles on a TFTR graphite tile exposed to D–D plasmas and a JET graphite tile from the first tritium campaigns were examined by full combustion, thermogravimetry and thermal desorption. Combustion measurements revealed that >98.9% of the tritium is trapped in a layer <50 μm thick, the remainder being spread throughout the tile. The tritium distribution on the tile surface is not homogeneous. A significant fraction resides in the gaps between tiles. Graphite disks from the plasma-exposed side of JET tiles heated up to 1100°C under a helium stream containing 0.1% hydrogen showed the highest tritium release rate at ~850°C. The agreement between tritium measurements by full combustion and thermal release was reasonably good. Tritium on graphite tiles was released to >95% under a stream of moist air at about 400°C. A large fraction of tritium can be removed from the tile surface with adhesive tape.

1. Introduction

A number of reactions capable of producing fusion energy are used in present day tokamaks [1]. These are:

$$D + D \rightarrow T + H + 3.98\ \text{MeV}, \quad (1)$$

$$D + D \rightarrow He^3 + n + 3.25\ \text{MeV} \quad (2)$$

and

$$D + T \rightarrow He^4 + n + 17.6\ \text{MeV}. \quad (3)$$

In the case of D–D plasmas (reactions (1) and (2)) some tritium is produced by reaction (1) and will hence be found at low levels in the unburned deuterium. Reaction (3) will only cause the removal of about 1% of the tritium. Since only a small fraction of the deuterium fuelled undergoes fusion reactions, the amount of tritium in the unburned deuterium is rather small. Because of plasma wall interactions a fraction of the fuelled deuterium becomes incorporated into the first wall materials of fusion machines. It is therefore expected that the wall materials will become tritium-contaminated.

To reduce the detrimental effect of impurities in the plasma, low Z materials are used as plasma-facing components. In most present day tokamaks, carbon is chosen because of its ability to withstand high heat fluxes, its high sublimation temperature and its relatively low erosion rate. During plasma discharges hydrogen isotopes are implanted into the graphite tiles as ions or as energetic charge exchange neutral atoms. Complex processes different to some extent from those known in

* Corresponding author.

0022-3115/00/$ - see front matter
PII: S0022-3115(00)00018-0

metals [2] govern the transport of hydrogen in graphite. Plasma particles interact not only with the outer surfaces but also with the inner surfaces of the interconnected pores. Hydrogen atoms may also be co-deposited with carbon, whereby the eroded carbon combines with the plasma to form a deposited amorphous, hydrogenated carbon film. Retention via co-deposition and implantation of energetic ions into the near-surface layers as well as bulk effects including migration through the network of interconnected pores and diffusion across the grains are dependent on the plasma operation conditions and on the degree of neutron and α irradiation damage [3]. It is known that hydrogen implanted at room temperature is retained at the near-surface until saturation is reached [4,5]. The saturation concentration has been reported to be in the H/C ratio range of 0.3–0.6 [6] and depends on the prevailing temperature (it decreases with increasing temperature) as well as on the implantation energy, being relatively insensitive to the microstructure of the carbon. While the thickness of the saturated layer is essentially given by the range of the most energetic particles, i.e. a few ten μm [7], there is in principle no limit to co-deposition. Whereas surface adsorption governs the retention at low temperatures, bulk migration and trapping predominate at elevated temperatures.

Several methods based on rather different principles have been used to investigate the profiles of tritium in graphite. Tritium imaging is frequently employed to analyse near-surface tritium. The method uses the primary β-rays of tritium, which cause the emission of secondary electrons from the material surface [8]. The image brightness is approximately proportional to the amount of tritium within 500 nm from the graphite surface. The detection limit for tritium by this technique is reported to be less than 10^{16} T/cm^2 [9]. Good results for depth profiling of tritium in graphite have also been obtained with a variety of nuclear physics methods [10,11]. Another approach to determine tritium in graphite consists in dissolving graphite specimens in chromo-sulphuric acid and analysing the distillate by a liquid scintillation counting technique [12]. This method, however, involves two steps, i.e. dissolution and distillation, and yields a tritium-contaminated liquid waste that is difficult to deal with. It is furthermore much less sensitive than a determination of tritium by full combustion [7].

In the present work, a quantitative determination of the depth concentration and surface concentration profiles of tritium in graphite tiles obtained from operating fusion machines was carried out by full combustion. In addition, thermal release rates of selected graphite specimens were measured. Specimens from tiles were taken at the Hot Cells and analysed at the Tritium Laboratory Karlsruhe (TLK), the Institute for Nuclear and Energy Technology (IKET), and the Institute for Instrumental Analysis (IFIA).

2. Experimental

2.1. Materials

The tiles available for the present study were:

- a virgin Ringsdorff graphite (EK98) and a carbon fibre composite (CFC) Dunlop tile from JET;
- a D–D plasma-exposed graphite tile from TFTR, Princeton;
- a D–T plasma-exposed Ringsdorff graphite (EK98) tile from JET.

The type EK98 (super pure) graphite tile from JET has a density of 1.85 g/cm^3, an open porosity of 10% and yields 5% ash. Typical impurities and their respective levels, as given by the manufacturer, are Al < 0.1, B 0.05, Ca 0.3, Co < 0.1, Cr < 0.1, Cu 0.1, Fe 0.3, Mg 0.05, K < 1, Mn < 0.1, Na < 1, Ni < 0.1, P < 0.3, S < 2, Si 0.5, Ti 0.3 and V 0.1 ppm, respectively. According to the manufacturer graphite is resistant in air up to temperatures of about 750 K. The graphite tile from TFTR was supplied through the European Fusion Program NET via JET.

2.2. Preparation of cylindrical graphite specimens and of disks for tritium analysis

For the preparation of cylindrical specimens a hollow drill was employed, with which specimens could easily be cut from selected zones of the various tiles. The cylinders obtained had a diameter of approx. 7.6 mm and a height corresponding to the thickness of the tile. Disks with a thickness of 1 mm were cut from the cylindrical specimens employing a diamond-grinding disk. The grinding disk was rotated with only 100 rpm to avoid unnecessary heating of the cylinder. To minimise cross-contamination, the diamond-grinding disk was cleaned after each cutting. Fig. 1 shows typical

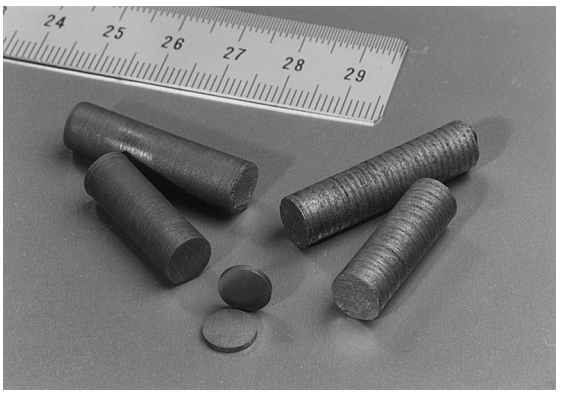

Fig. 1. Cylindrical specimens and disks from Ringsdorff EK98 graphite (darker) and CFC (metallic appearance, striated) obtained from virgin JET graphite tiles.

cylinders and disks prepared from virgin graphite and virgin CFC tiles supplied by JET. The disks were each numbered and placed in a single flask. Disks from the plasma facing side of the tile were numbered beginning with A1 up to AN and disks from the opposite side beginning with B1 up to BN, always starting from the tile surface.

To allow a gapless determination of tritium depth profiles, two cylinders from a JET tile were cut from immediately neighbouring zones of the tile and disks from alternating depths were cut from both cylinders (see Fig. 2). Under the assumption that closely neighbouring cylinders have a comparable concentration distribution, a reliable tritium depth profile in 1 mm depth steps can be obtained.

2.3. Methods for sample characterisation

2.3.1. Thermogravimetry

For the thermogravimetric analysis (TGA) and differential thermal analysis (DTA) of graphite disks or their fragments a Netzsch STA409 thermobalance equipped with a PU 1.851.01 power unit and a TASC414/3 controller was employed. Temperatures were measured with a PtRh10-Pt thermocouple placed axially at the bottom of the ceramic sample holder. The instrument allows heating of the sample up to a temperature of 1300°C. Heat treatments were carried out either under inert gas (argon or nitrogen), air, or vacuum. In runs with samples containing tritium the exhaust gas was passed through bubblers with water.

2.3.2. Combustion

The technique proposed by Vance et al. [13] was followed for graphite combustion. The experimental glass apparatus used at the TLK is shown schematically in Fig. 3. Either a stream of laboratory air pumped with an oil-free Metal Bellows pump type MB 158E or pure air from a pressurised cylinder was used with a flow rate of approx. 15 cm^3/min. Passing the air through a bubbler containing water humidified the carrier gas. Graphite or CFC disks were introduced via a joint into a small receptacle placed on top of the combustion zone and isolated from this zone by a glass-to-glass seal. To introduce the graphite disk into the combustion zone the seal was lifted from the outside with two appropriate magnets. The combustion zone itself consists of a vertically arranged quartz tube heated from the outside with a cylindrical Ströhlein oven designed for temperatures up to 1500°C. The actual sample temperatures were determined with a thermocouple placed inside the quartz tube. The combustion tube itself contained approx. 20–30 g of a wire packing consisting of a Cu_2O core with CuO on the surface supplied by Merck, Darmstadt. The packing is secured between two pieces of quartz wool packing, on top of which the disk to be analysed drops by gravity when the seal is open. The copper oxide contributes to ensure complete oxidation of all molecular hydrogen isotopes and all hydrocarbons released during the combustion of the disks. The effluent gases are then passed through a bubbler containing water (about 50 cm^3) via the shortest route. By this procedure the quartz tube, extending from the

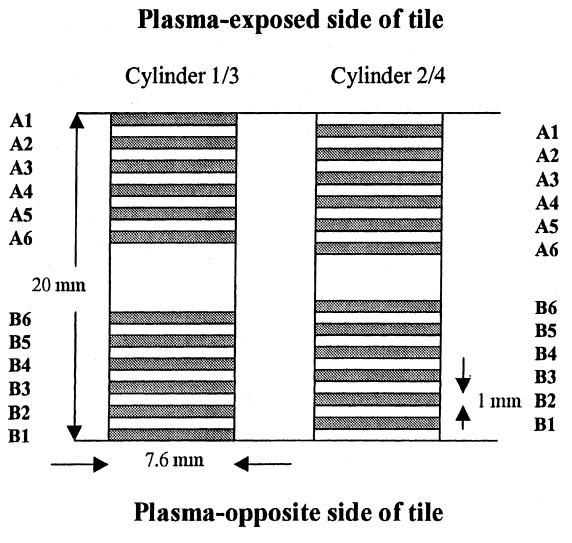

Fig. 2. Numbering of the disks obtained from cylinders No. 1–4 drilled from the plasma-exposed side of the TFTR graphite tile.

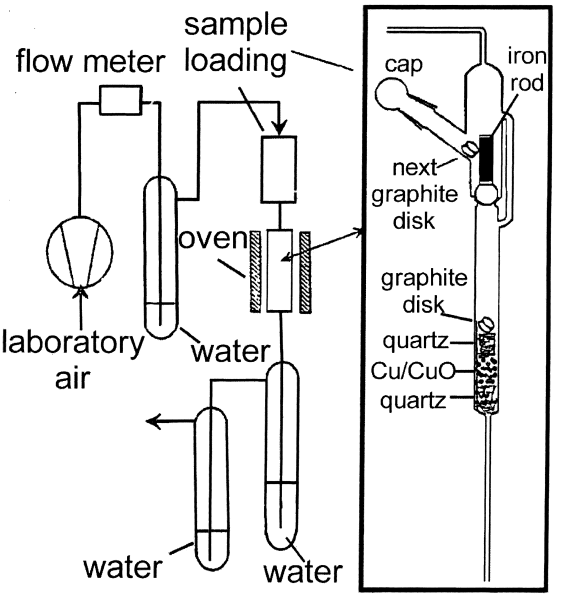

Fig. 3. Schematic view of the glass apparatus employed for the combustion of graphite and CFC disks.

combustion zone down to the water level in the bubbler, remains at all times at comparatively high temperature. The experimental evidence indicates that most of the tritiated water is retained in this bubbler. To assure quantitative trapping of the tritiated water, a second bubbler, also filled with water, was placed downstream.

After each combustion, 1 cm^3 water aliquots were taken from each of the bubblers employing calibrated syringes. These aliquots were mixed with 15 cm^3 of a scintillation cocktail and analysed for total tritium with a liquid scintillation counter (LSC). The LSC instrument employed at the TLK is a Tri-Carb 2300TR Liquid Scintillation Analyser from Packard. Upon completion of an analysis, the surface contamination remaining on the tubing inserted into the water of the first bubbler was removed by rinsing thoroughly several times with fresh water. Frequent blank tests without sample or with virgin graphite disks were carried out to verify that no cross-contamination had taken place.

Typical results obtained with a single A1 disk (mass 27.60 mg, diameter 7.7 mm and thickness 1 mm) cut from cylinder No. 6 of the TFTR graphite tile and heated up to 850°C under a moist air stream of 10 cm^3/min were 16.1 ± 0.4 Bq/cm^3 in the first bubbler and 0.3 ± 0.0 Bq/cm^3 (comparable to background levels) in the second bubbler. As a rule, to achieve good statistics, six water aliquots were pipetted from each bubbler and each of the prepared scintillation cocktails was counted three times. The tritium measurements demonstrate that more than 98% of the liberated tritium is collected in the first bubbler. The high tritium retention in the first bubbler is achieved with glass filters of very small pores, i.e. 160–250 μm, at the tip of the inlet tube to the bubbler. Under these conditions very fine gaseous bubbles are generated and a very good HTO/DTO retention in the water of the bubbler is achieved. Generally, the reproducibility of the tritium concentration in the six water aliquots was found to be much better than 5%.

At IFIA a similar arrangement as that described above was employed to burn the disks. The liquid scintillation counter used in this case was from Philips PW4700. The samples were also burned in a vertically arranged quartz tube. Instead of air, however, a stream of humidified oxygen at a flow rate of 50 cm^3/min was used for the oxidation. From the literature it is known that the rate of oxidation is increased by 60% when air is replaced by oxygen [4]. The combustion quartz tube contained about 29 g of copper oxide wire arranged in the same manner as described above. Heating was carried out with a cylindrical oven capable of attaining temperatures as high as 1500°C. The effluent combustion gases were passed through water in a bubbler placed in an ice bath. After a certain collection period the bubbler was replaced with a fresh one. To minimise cross contamination from one measurement to the other, an immersion tube without a glass filter was used. As a rule two flasks were sufficient to collect the tritium quantitatively. Occasionally, approx. 10–15% of the total activity were retained in the second bubbler. Two aliquots were taken from each bubbler and five counting cycles were carried out to achieve good statistic.

A white residue (ash) remained when graphite was fully burned at temperatures below 800°C. The residue, which had the same shape as the initial disk, i.e. circular, was very thin and found to weigh less than 0.1% of the weight of the starting material. A chemical analysis of the residue yielded silicon and aluminium as main constituents. No ash was found in the reactor after burning CFC samples.

2.3.3. Thermal desorption

The desorption studies were performed with a laboratory facility installed at IKET. The experimental setup basically comprises a purge gas supply and control, a high temperature stainless steel chamber containing the sample, a reduction bed containing granulated zinc operated at approx. 390°C and a calibrated proportional counter for the detection of tritium. The sample chamber is heated from the outside with a controllable tubular furnace. The zinc bed converts tritiated water to molecular gaseous tritium (HT, DT, and traces of T_2). The tubing downstream of the ionisation chamber is trace-heated to about 300°C. This heating contributes to minimise memory effects caused by tritiated water. Except for the pure gas supply and control, the whole system is contained in a glove box.

The purge gas used was helium containing 0.1 vol.% hydrogen. Typical flow rates were 50 cm^3/min. In normal operation, the sample temperature is initially increased linearly with time (reference rate 5 K/min) up to an end temperature of max. 1100°C, which is kept constant for a pre-determined time.

The purge gas flow rates, the sample temperatures and the tritium activity in the purge gas, which is derived from the count rate of the proportional counter, are continuously measured and registered. The registered data are processed and evaluated with a PC data acquisition system. The count rate is corrected for the system background as determined at the start and the end of each run (sample at room temperature). The tritium release from the sample is obtained from the corrected count rate and the measured flow rate. The total released activity is calculated by integrating the release rate over the time region where a release is measurable.

3. Results and discussion

3.1. Results from TGA and DTA analysis

To determine optimised conditions for the combustion of graphite and of CFC specimens thermogravi-

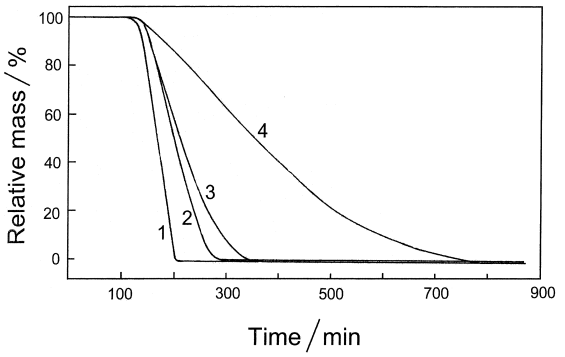

Fig. 4. Thermogravimetry of various CFC and graphite samples at progressively increasing temperatures. The curves show the rate of mass loss of (1) graphite at 800°C, (2) CFC at 780°C, (3) CFC at 750°C, and (4) CFC at 700°C, respectively.

metric experiments were first carried out with blanks under laboratory air. Fig. 4 depicts the isothermal combustion of CFC and of graphite disk segments at temperatures between 700°C and 800°C. From the results it is apparent that a rapid combustion can only be achieved at very elevated temperatures. For instance, for the complete oxidation of a 34 mg graphite sample at 800°C, a total burning time of approximately 2 h is required. At temperatures only 100 degrees less, the combustion time for only 22.8 mg of CFC increases significantly to more than 12 h.

Visual inspection showed that under the employed conditions CFC leaves no residue after a complete combustion at 850°C. Conversely, a small grey residue remained in the ceramic crucible when a graphite disk was burned under the same temperature program.

Fig. 5 compares thermogravimetrically, under identical experimental conditions, the burning of graphite

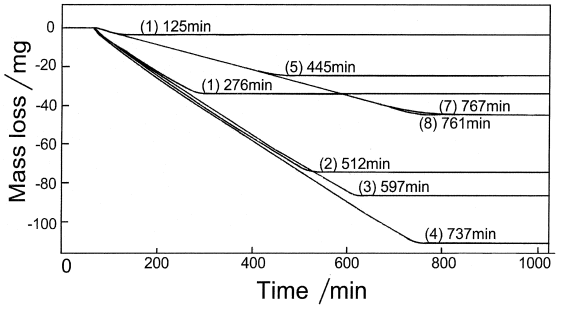

Fig. 5. Time required to burn isothermally increasing amounts of graphite disk fragments at a temperature of 780°C. Curve (1) shows the heating of 33.5 mg, curve (2) of 73.75 mg, curve (3) of 85.70 mg and curve (4) of 109.95 mg graphite, respectively, for the indicated total combustion time. Curve (6) shows the heating of 3.5 mg, curve (5) of 24.15 mg, curve (7) of 43.65 mg and curve (8) 43.90 mg CFC, respectively, for the indicated total combustion time.

and of CFC. The samples were heated at a rate of 10 K/min up to a final temperature of 780°C, which was thereafter held constant for about 15 h. From the slopes of the straight lines weight loss rates of (9.5 ± 0.4) mg/h and (3.8 ± 0.3) mg/h were estimated for pure graphite and CFC, respectively. Thus it is apparent that graphite oxidises much more readily than CFC. The time for the complete combustion of pieces from a disk is roughly directly proportional to the increase in sample weight (see Fig. 6). For instance, while the burning of 24.15 mg of CFC is completed in about 400 min, that of 43.65 mg requires about 700 min. In both cases the combustion rate is nearly the same, i.e. 3.8 mg/h. This suggests that the rate of combustion is determined by the exposed surface (grinding of the pieces would of course give rise to another rate).

A comparison under vacuum and under air of the TGA and the DTA of graphite is illustrated in Fig. 7.

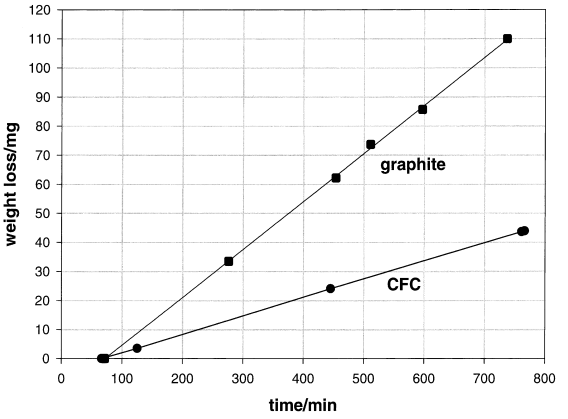

Fig. 6. Time required to burn isothermally at 780°C increasing amounts of graphite disk and CFC disk fragments.

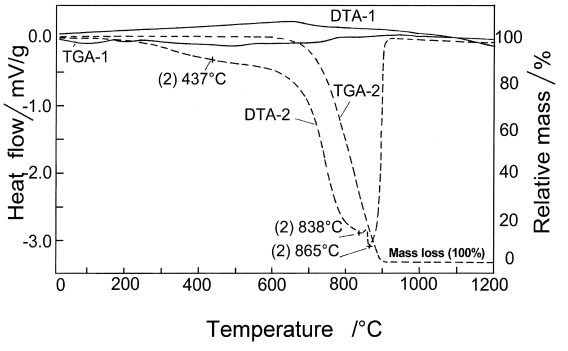

Fig. 7. Comparison between the thermogravimetric analysis of graphite under air (TGA-2, broken line) and under vacuum (TGA-1, solid line) and comparison between the differential thermal analysis of graphite under air (DTA-2, broken line) and under vacuum (DTA-1, solid line).

When a sample of 14.85 mg of virgin graphite was heated up to 1300°C under air atmosphere at a rate of 5 K/min, the sample oxidised with a progressively increasing weight loss rate after the temperature reached values higher than 650°C. Complete oxidation took place after approx. 3 h and 890°C. The endothermic DTA peak observed at approx. 437°C is probably not due to a graphite re-crystallisation or phase transformation (a phase transformation has been reported at >1025°C by Greenwod et al. [14]). On this account the DTA peak below 600°C is attributed to oxygen chemisorption reactions leading to the formation of oxide surface complexes [15]. The broad endothermic DTA peaks registered during the oxidation phase with maxima at 838°C and 865°C, suggests that the oxidation of graphite yielding gaseous products takes place in more than one reaction pathway. Potential reactions include:

$$2C(s) + O_2(g) \rightarrow 2CO\ (g), \tag{4}$$

$$C(s) + O_2\ (g) \rightarrow CO_2(g). \tag{5}$$

3.2. Determination of total tritium in graphite disks by full combustion

Full combustion was employed to determine the tritium content in graphite disks from TFTR and JET tiles. Reactions (4) and (5) of graphite with oxygen in the temperature range 600–800°C are known to be one half order with respect to the partial pressure of oxygen, and are essentially pore diffusion controlled. Primary products of the reaction are carbon monoxide and carbon dioxide. Whereas CO_2 is predominantly formed at low temperatures, i.e. 500°C, the most important product at higher temperatures is CO. With increasing temperatures the CO/CO_2 ratio rapidly increases and goes through a maximum. Above 800°C the gas phase reaction

$$2CO(g) + O_2\ (g) \rightarrow 2CO_2(g) \tag{6}$$

must be included in the reaction scheme.

There are experimental indications that the presence of moisture is necessary for the full combustion of charcoal [16]. For the quantitative determination of tritium in a solid by full oxidation a moist carrier gas is also recommended to minimise memory effects. Therefore, it is necessary to contemplate the reactions of carbon and carbon oxides with steam. The first step when water vapour and carbon are brought in contact involves the adsorption of water on the carbon surface. This adsorption will occur even at temperatures as high as 700°C. This step is followed by the evolution of carbon monoxide, carbon dioxide, and hydrogen from the solid. The overall reaction can be described by [15,17]

$$H_2O\ (g) + C(s) \rightarrow H_2\ (g) + CO\ (g), \tag{7}$$

$$2H_2O\ (g) + C(s) \rightarrow 2H_2\ (g) + CO_2\ (g), \tag{8}$$

$$H_2O\ (g) + CO\ (g) \rightarrow H_2\ (g) + CO_2\ (g), \tag{9}$$

the oxygen in this oxidation path being supplied by water. At elevated temperatures the Boudouard equilibrium

$$CO_2\ (g) + C(s) \rightarrow 2CO\ (g) \tag{10}$$

also needs to be included in the mechanism.

In the following, the combustion results obtained with samples from a TFTR and a JET tile are discussed in detail.

3.2.1. TFTR tile

As mentioned in a previous section, a stream of moist air (or oxygen) is used for the oxidation of the tritium-containing graphite specimens. The results on the depth profile of tritium in a TFTR tile exposed to a D–D plasma are compiled in Table 1. The data were obtained from the disks of cylinders 1, 2, 3 and 4 (see Figs. 2 and 8). The agreement between the tritium content measurements performed at IFIA and the TLK is quite satisfactory, particularly when considering that two neighbouring cylinders do not necessarily have to have equal tritium concentrations at the surface and bulk zones. In addition, it is seen that most of the tritium (probably >98%) is found within a depth of max. 1.5 mm (1 mm disk thickness plus 0.5 mm cut) from the tile surface exposed to the plasma (approx. 6 kBq/cm^2 in a disk specimen of 0.45 cm^2 and 1 mm thickness). Since the cuttings between disks, corresponding to a virtual disk of about 0.45 mm thickness, could not be analysed, it is not possible on the basis of these results to define with certainty what fraction of tritium is actually retained in the first mm. In other words, it is not possible to indicate precisely what the actual depth from the surface is that contains most of the tritium (possibly only a few micrometers). All other disks from zones deeper into the cylindrical specimen, i.e. >1.45 mm, yielded tritium activities of the order of the background level or very slightly above.

The observed high concentration of tritium in the near-surface zone agrees well with previous observations with JET tiles by other investigators [18,19]. Peacock et al. [18] reported that 98% of the tritium (6.8×10^4 Bq/cm^2) is trapped within a depth of 4 mm of the plasma facing surface layer of a JET tile exposed to plasma's containing up to 1.3% tritium. Their investigation also indicated that tritium at low levels is present throughout the tile (of the order of 0.4–0.7 $\times 10^3$ Bq in specimens of 4 mm thickness and 1.04 cm^2 surface area, obtained at increasing depths into the tile). Pontau et al. [19] reported that most of the deuterium–tritium is

Table 1
Depth profile of tritium in a TFTR graphite tile

Disk	Measurements at TLK			Measurements at IFIA		
	1st bubbler (Bq/g)	2nd bubbler (Bq/g)	Total activity (Bq/g)	1st bubbler (Bq/g)	2nd bubbler (Bq/g)	Total activity (Bq/g)
	Graphite cylinder No. 2			*Graphite cylinder No. 1*		
A1	37610.8	99.5	37710.3	32005.8	4712.8	36718.6
A2	8.1	4.0	12.1	4.0	7.3	11.2
A3	–	–	–	8.5	5.5	13.9
A4	21.8	7.9	29.7	5.6	12.3	17.8
A5	–	–	–	29.2	5.6	34.8
A6	–	–	–	8.5	7.4	15.9
B6	–	–	–	7.8	17.3	25.1
B5	–	–	–	7.4	6.8	14.2
B4	–	–	–	12.4	7.9	20.3
B3	–	–	–	0.0	9.0	9.0
B2	–	–	–	5.8	0.0	5.8
B1	–	–	–	1.3	7.6	8.9
	Graphite cylinder No. 4			*Graphite cylinder No. 3*		
A1	5599.5	131.8	5731.3	6980.1	79.2	7059.3
A2	155.4	12.3	167.7	34.7	7.9	42.6
A3	–	–	–	38.8	8.7	47.5
B3	–	–	–	16.1	13.0	29.1
B2	–	–	–	1.7	9.5	11.2
B1	–	–	–	56.5	3.3	59.8

located within a μm depth range from the graphite surface of samples exposed to a deuterium–tritium plasma in a discharge apparatus that simulates conditions existing at the plasma edge of a fusion device. Further experiments described below performed with the JET tiles validate these earlier observations.

In another study, the surface homogeneity of the tritium on the plasma-exposed side of the TFTR graphite tile was examined more closely. Altogether seventeen cylinders were drilled from the tile as shown in Fig. 8 and the tritium content in the corresponding A1 disks (plasma-exposed side disk) of eleven of them were measured partly at IFIA and partly at TLK employing the combustion method (see Table 2). From the data it is apparent that A1 disks from graphite cylinders drilled out of the TFTR tile from closely neighbouring sites have very similar tritium concentrations. The tritium distribution on the whole surface of the tile on the other hand, is not homogeneous and can vary by a factor of up to 11.

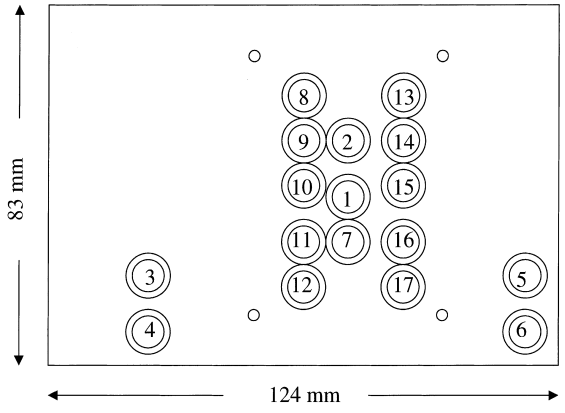

Fig. 8. Sample points of a plasma-exposed TFTR graphite tile. The numbers are identical with those given in Table 2.

The tritium concentration of the D–D plasma-exposed TFTR tiles was found to be of the order of 10^{12}–10^{13} T/cm^2 [18] (in plasma operation with an equimolar deuterium–tritium mixture activities of the order of 5×10^{17} T/cm^2 are expected [9,20]). Based on the measurements carried out at FZK with a single TFTR tile an average value of $(5.3 \pm 1.8) \times 10^{12}$ T/cm^2 (extrapolated back to 1989, when the measurements were performed by Causey et al. [21]) was found, which is of the same order of magnitude as reported in [21]. A similar average value (5.8×10^{12} T/cm^2) was estimated for tiles employed during the D–D operation of JT60U [22]. Taking into account that the tritium concentration in tiles will depend upon the position of the tile inside of the machine and the subsequent wall treatments inside of the machine before the tile is removed, the agreement between the observed values can be considered good.

It is worthwhile to point out that the tritium accumulated in the graphite during the operation of the

Table 2
Distribution of tritium at the surface of a TFTR tile exposed to a D–D plasma

Cylinder No.	Sample weight (mg)	Absolute activity (Bq)	Atomic activity (T/cm^2)[a]	Atomic activity (T/cm^2)[b]	Surface activity (kBq/cm^2)
1[c]	69.30	2543	3.15×10^{13}	4.93×10^{12}	5.60
2[d]	77.85	2926	3.63×10^{12}	5.68×10^{12}	6.44
3[c]	79.09	559	0.69×10^{12}	1.08×10^{12}	1.23
4[d]	79.65	445	0.55×10^{12}	0.86×10^{12}	0.98
5[d]	37.30	1739	4.04×10^{12}	6.34×10^{12}	7.20
6[d]	27.60	799	2.69×10^{12}	4.21×10^{12}	4.78
7[d]	35.65	2010	5.56×10^{12}	8.72×10^{12}	9.90
8[d]	33.70	1028	2.74×10^{12}	4.30×10^{12}	4.88
9[d]	79.30	2345	2.90×10^{12}	4.55×10^{12}	5.17
16[d]	79.40	4158	5.14×10^{12}	8.07×10^{12}	9.16
17[d]	73.10	5046	6.24×10^{12}	9.79×10^{12}	11.11
Average			$(3.39 \pm 1.82) \times 10^{12}$	$(5.32 \pm 1.82) \times 10^{12}$	(6.04 ± 3.23)

[a] Total activity measured in A1 disk expressed per cm^2 of plasma-exposed side (the disk having a surface area of approx. 0.45 cm^2).
[b] Atomic activity retro-dated to the measurements in [20].
[c] Analysed at the IFIA.
[d] Analysed at the TLK.

fusion machine after completion of all wall cleaning procedures is firmly sequestered in the tiles.

3.2.2. Jet graphite tile

For tritium analysis a large number of cylinders were cut from JET tile 004/2.20 according to the scheme illustrated in Fig. 9. A total of twelve equal sized disks (7.6 mm diameter and 1 mm thick) were cut from each side of the cylinders 2, 8, 16 and 17. As opposed to measurements with the TFTR disks a yellow/brown deposit at the exit of the quartz combustion tube was noticed when the B disks from JET were burned. Upon closer examination it was confirmed that the deposit originated from pump oil (the original Metal Bellows pump had failed and been replaced by an oil-lubricated pump). The oil-lubricated pump was therefore substituted by a pressurised cylinder containing synthetic air. Subsequent to this improvement the deposit no longer appeared. The results from the combustion of all disks from cylinders 17, 2, 8 and 16 are compiled in Tables 3 and 4. To narrow down on the tritium depth profile, disks from graphite cylinder No. 17 and 8 were cut starting at the plasma-exposed surface and disks from graphite cylinder No. 2 and 16 starting 1 mm below the plasma-exposed surface. The A1, A2 and A3 disks from cylinders 17 and 2 were combusted using synthetic air instead of the oil-lubricated compressor. The disks from graphite cylinders No. 8 and No. 16 were combusted using pure oxygen.

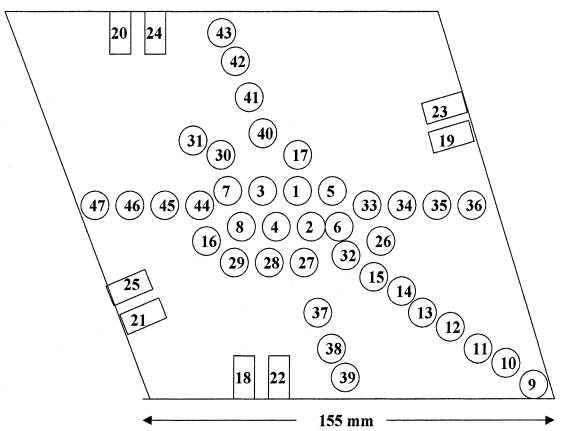

Fig. 9. Sampling map of JET tile 004/2-20 showing the positions of the cylinders cut from the plasma-exposed side of the tile (cylinders 1–17) and the lateral side of the tile (cylinders 18–25).

Analogous to the findings with the TFTR tile, the results given in Tables 3 and 4 for cylinders 8 and 17 of JET tile 004/2-20 indicate that more than $(98.9 \pm 0.2)\%$ of the tritium (tritium immobilised in the gaps between the tiles was also taken into account by interpolation) is trapped within the first mm in depth. Since the A1 disk of cylinder No 2 (collected 1 mm below the surface) does show a somewhat higher tritium activity than the rest either a small tritium fraction penetrated into the tile up to a depth of more than 1 mm or during the cutting of the disks some tritiated graphite was smeared from one disk to another. From the above it appears that a small fraction of tritium, i.e. <1.1%, is uniformly distributed throughout the tile.

In Table 5 the concentration of tritium in 1 mm thick disks taken from various zones of the plasma-exposed surface of JET tile 004/2-20 is compared. The positions of the disks are shown in Fig. 9. As can be seen, with one exception, most of the tritium is collected in the first bubbler. The average concentration of tritium in JET tile 004/2-20 was determined to be (13.8 ± 3.5) kBq/cm^2. This activity concentration corresponds to the tenaciously

Table 3
Tritium depth profile of JET graphite tile 004/2-20 measured by the combustion technique at the TLK

Disk	Graphite cylinder No. 17[a]				Graphite cylinder No. 2[b]			
	1st bubbler (%)	2nd bubbler (%)	Actual activity (Bq/g)	Tritium activity (Bq/cm^2)[c]	1st bubbler (%)	2nd bubbler (%)	Actual activity (Bq/g)	Tritium activity (Bq/g)
A1	98.1	1.9	69 251.2	12 324.9	99.8	0.2	231.7	42.4
A2	99.6	0.4	356.0	66.1	99.8	0.2	22.4	3.8
A3	99.6	0.4	20.9	3.9	99.7	0.3	65.9	11.6
A4	99.7	0.3	49.5	8.8	99.4	0.6	35.3	6.0
A5	99.7	0.3	87.4	16.0	99.8	0.2	176.0[d]	30.8
A6	99.8	0.2	15.2	2.7	100.0	0.0	34.6	6.1
B6	99.8	0.2	24.4	4.4	–	–	–	–
B5	99.6	0.4	24.6	4.4	99.8	0.2	45.2	7.7
B4	99.7	0.3	18.4	3.3	99.5	0.5	64.3	11.5
B3	99.5	0.5	24.7	4.4	99.3	0.7	31.0	5.5
B2	99.6	0.4	21.1	3.9	99.6	0.4	16.8	2.9
B1	99.7	0.3	108.0	18.2	99.8	0.2	199.7	36.3

[a] The disks of cylinder No. 17 were cut starting at the plasma-exposed surface of the cylinder.
[b] The disks of cylinder No. 2 were cut starting one mm below the plasma-exposed side of the cylinder.
[c] Activity expressed in Bq per cm^2 of plasma-exposed surface after background correction.
[d] The high tritium value is attributed to a cross contamination from disk A_1 of cylinder No. 6, which was analysed between disks A_4 and A_5.

Table 4
Tritium determination in graphite disks from cylinders 8 and 16 form JET tile 004/2-20. The measurements were carried out at IFIA by combustion and liquid scintillation counting

Cylinder No.	Disk No.	Disk weight (mg)	Released tritium first fraction (Bq/g)	Released tritium second fraction (Bq/g)	Total activity[a] (Bq/cm^2)
16	A1	77.07	28.5	48.2	13.0
16	A2	77.74	78.0	19.5	16.7
16	A3	76.70	30.0	37.5	11.4
16	A4	78.17	26.8	13.0	6.8
16	A5	79.46	47.2	14.2	10.8
16	A6	78.42	25.2	17.1	7.3
16	B1	84.48	59.2	54.6	21.2
16	B2	83.07	34.1	6.0	7.3
16	B3	80.80	58.2	46.9	18.7
16	B4	78.37	78.0	12.4	15.6
16	B5	80.61	48.0	88.7	24.3
8	A1	81.50	80191.7	161.8	14424.7
8	A2	84.80	25.9	16.7	8.0
8	A3	82.56	115.4	25.7	25.6
8	A4	81.06	28.5	18.9	8.5
8	A5	81.32	35.9	36.2	12.9
8	A6	82.26	202.2	18.3	39.9
8	B1	77.00	16.2	11.7	4.7
8	B2	81.35	20.7	3.2	4.3
8	B3	82.51	15.1	24.4	7.2
8	B4	79.81	121.2	26.1	25.9
8	B5	80.89	87.9	19.9	19.2
8	B6	80.13	31.8	31.4	11.1

[a] Activity expressed in (Bq/cm^2) of plasma-exposed surface.
[b] The disks of cylinder No. 16 were cut starting 1 mm below the plasma-exposed of the cylinder.

Table 5
Distribution of tritium on the plasma-exposed surface of JET tile 004/2-20 (for sample mapping see Fig. 9)

Cylinder No.	Laboratory	Disk mass (mg)	Total activity (Bq)	Activity in the 1st bubbler (%)	Activity in the 2nd bubbler (%)	Surface activity (kBq/cm^2)
(a) *1 mm thick A1 disks*						
1	TLK	78.90	7409	100	0.0	16.3
8	IFIA	81.50	6549	99.8	0.2	14.4
9	TLK	85.70	2958*	100.0	0.0	6.5
10	TLK	78.85	5636	95.5	4.5	12.4
11	TLK	75.80	7964	98.6	1.4	17.5
12	TLK	81.55	5008	100.0	0.0	11.0
13	TLK	80.40	7136	85.0	15.0	15.7
14	TLK	81.70	7120	97.5	2.5	15.7
15	TLK	81.10	6872	97.4	2.6	15.1
17	TLK	80.80	5595	98.0	2.0	12.3
37	TLK	78.50	10 233	99.9	0.1	22.5
38	TLK	78.10	5249	97.3	2.7	11.6
39	TLK	79.60	6044	99.4	0.6	13.3
44	TLK	81.40	6660	99.5	0.5	14.7
45	TLK	74.00	4766	96.5	3.5	10.5
46	TLK	70.40	5950	100.0	0.0	13.1
47	TLK	45.20	6591	100.0	0.0	14.5
Average		77.3 ± 9.0	6588 ± 976			13.8 ± 3.5
(b) *0.53 mm thick A7 disks*						
2	IFIA	43.38	7616	99.7	0.3	16.8
4	TLK	45.10	7707	99.5	0.5	17.0
6	IFIA	41.39	3220	99.9	0.1	7.1
16	TLK	40.60	6603	99.7	0.3	14.5
Average		42.62 ± 2.03	6287 ± 2105			13.9 ± 4.6

held inventory resulting from the integrated effect of numerous discharges at JET and the subsequent wall cleaning steps. In general, the surface-near concentrations vary within a factor of more than three. This may be caused by an inhomogeneous magnetic field in the machine, by an inhomogeneous co-deposition or losses during the tile handling while they were removed from the machine or during their subsequent interim storage. More tritium determinations presently under way with CFC tiles from the DTE1 campaign of JET will provide further information concerning the distribution of the tritium concentration on tile surfaces and in the bulk.

Employing tritium imaging it was observed that upon sputtering JET tiles with 5 keV Ar^+ ions, a very substantial decrease in brightness takes place after a sputtering depth of approx. 350–500 nm [8]. This points to an even steeper and narrower tritium depth profile of the JET tiles than that derived from the present measurements. Experiments performed by Goodall et al. [7], who removed slices of graphite with an abrasive paper from an inner wall tile of JET, support this observation.

Four 0.53 mm disks, here designated as A7 disks obtained from cylinders cut to 1 mm below the surface (0.53 + 0.47 mm cut), were also analysed for tritium (see Table 5(b), bottom). From the fact that the four investigated disks had practically the same weight, it can be concluded that their thickness was closely comparable. The average total activity obtained, i.e. (13.9 ± 4.6) kBq/cm^2, essentially corresponds to that found in the 1 mm A1 thick disks taken from the tile surface. One can therefore conclude that the bulk of the activity is concentrated in a tile depth of less than 0.5 mm. Results for the A7 disks expressed in kBq/cm^2 are within the error limits the same as the A1 disks (compare Table 5(a) and (b)).

To obtain more information on the depth profile a few cylinders were progressively eroded and the activity in the 'plasma-exposed' 1 mm disk obtained from the remaining cylinder analysed for tritium (see Table 6). It is seen that already after an erosion of 50 μm the tritium concentration drops to nearly background levels. From this it is clear that the co-deposited layer must be thinner than 50 μm. Recent tritium depth profiling measurements by accelerator mass spectrometry performed by Friedrich et al. [23] substantiate this observation. For an inner wall divertor tile, they found a total depth profile thickness of 25 μm having a maximum concentration at approximately 2 μm [11].

The results given in Table 7 obtained from the 'plasma-exposed' disks of cylinders cut from lateral sides of the tile demonstrate that tritium is also co-deposited

Table 6
Tritium depth profile in JET tile No. 004/2-20 obtained by progressive surface erosion. The data give the tritium in a 1mm thick disk immediately adjacent to the eroded surface

Sample No.	Laboratory	Eroded layer (μm)	Mass (mg)	Total activity (Bq)	Activity in first bubbler (%)	Activity in second bubbler (%)	Surface activity (Bq/cm^2)
27	TLK	70	86.65	30	100.0	0.0	70
29	TLK	60	85.00	41	100.0	0.0	90
28	IFIA	60	84.82	149	91.1	8.9	330
26	IFIA	50	87.41	11	89.7	10.3	20

Table 7
Tritium concentration on the lateral sides of JET tile 004/2-20. Results from plasma-exposed 1 mm thick disks

Cylinder	Disk mass (mg)	Total activity (Bq)	Activity in the 1st bubbler (%)	Activity in the 2nd bubbler (%)	Surface activity (kBq/cm^2)
18[a]	70.10	16.3	100.0	0.0	0.0358
22[b]	85.30	31.7	81.9	18.1	0.0696
19[a]	84.15	826.8	98.9	1.1	1.821
23[b]	79.56	801.2	99.3	0.7	1.765
20[a]	70.85	2110.0	97.9	2.1	4.648
24[b]	75.89	1777.0	99.7	0.3	3.914
21[a]	83.00	2510.0	99.5	0.5	5.529
25[b]	86.20	1890.8	99.5	0.5	4.165
Average	79.38 ± 6.42				

[a] Analysis at the TLK.
[b] Analysis at the IFIA.

on the side walls. The concentrations, which reached values as high as 5.5 kBq per cm^2 of plasma-exposed surface area, show a marked dependence from the position at which the sample was taken. Evidently the size and shape of the gaps between the tiles in the reactor as well as the access to the plasma play a role.

3.3. Tritium removal with an adhesive tape

In a few runs, the co-deposited layer was removed employing an adhesive tape. The tape was applied three times to the plasma-exposed surface of graphite cylinders of 7.6 mm diameter drilled from JET tile No. 004/2-20 and then combusted together with the adhered co-deposit. The results given in Table 8 clearly indicate that a very large fraction (25–50%) of the co-deposited layer can be easily removed by this procedure.

3.4. Determination of thermal tritium release rates

All tritium release rate measurements with disks from JET tile No. 004/2-20 were performed in the laboratories of the IKET. To improve the signal to background ratio in this thermal desorption investigation a low purge of He with 0.1% H_2 flow rate of 10 standard cm^3/min was used. To study the thermal release the sample temperature was raised up to 1100°C employing a rate of 5°C/min.

Altogether five disks from JET tile No. 004/2-20 were heated under isochronal conditions and the results summarised in Table 9. Only the disks obtained from the plasma-exposed side of the tile showed a significant tritium content of approximately 18–21 kBq per cm^2 of plasma-exposed surface. All other disks yielded tritium concentrations that were below the detection limit, i.e. 1.10 kBq/cm^2. Taking into account that the technique employed at IKET differs considerably from the one used at TLK and is probably less accurate because it is based on a calibrated proportional counter, the determined tritium concentrations are in reasonable agreement with the results given in Table 5.

The sample temperature, the tritium release rates and the total tritium released from the A1 disks of cylinders 5 and 7 are depicted in Figs. 10 and 11, respectively. The two release curves are essentially similar, i.e. the release commences at about 700°C, and the release rate reaches a maximum at approx. 850°C. At still higher temperatures the release rate decreases rapidly. When a maximum temperature of about 1100°C is attained the release rate drops to nearly zero; indicating that most of the tritium has gassed off. Similar observations have been reported by Sawicki et al. [24]. The higher peak release rates are possibly caused by the higher heating rates employed by these investigators. Of significant consequence to the development of detritiation methods could be their observation that neither a shift nor a broadening of the tritium depth profile could be detected

Table 8
Fraction of tritium removable from the tile surface with an adhesive tape

Sample No.	Laboratory	Mass of tape (mg)	Total activity (Bq)	Activity in first bubbler (%)	Activity in second bubbler (%)	Surface activity removed with adhesive tape (Bq/cm^2)
28	IFIA	51.22	3134	95.3	4.7	6900
29	TLK	49.90	1507	99.2	0.8	3300

Table 9
Thermal desorption measurements from JET graphite tile No. 004/2-20

Cylinder No.	Disk No.	Mass (g)	Released tritium[a] (Bq)	Surface activity (kBq/cm^2)
5[b]	A1	0.0792	9.516×10^3	20.96
	A2	0.0606	$\leqslant 5 \times 10^{2c}$	$\leqslant 1.10$
	B1	0.0819	$\leqslant 5 \times 10^{2c}$	$\leqslant 1.10$
6[d]	A1	0.0785	$\leqslant 5 \times 10^{2c}$	$\leqslant 1.10$
7[b]	A1	0.0791	8.293×10^3	18.27

[a] Integrated between 2650 s ($\approx$600°C) and 10400 s ($\approx$1100°C).
[b] A1 disks cut from cylinders No. 5 and No. 7 include the tile surface.
[c] Detection limit.
[d] A1 disk cut from cylinder No. 6 was obtained from 1 mm below the tile surface.

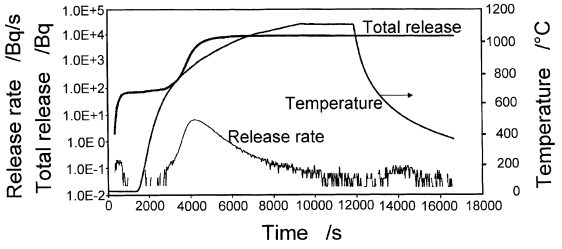

Fig. 10. Tritium release by thermal desorption from disks obtained from JET tile 004/2-20 (disk A1 from cylinder 5).

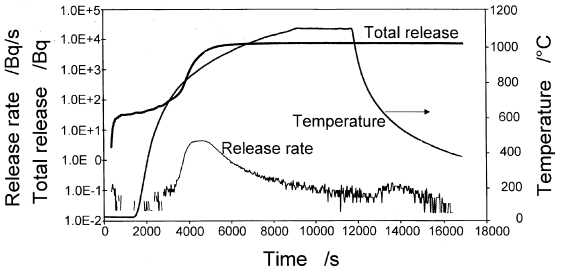

Fig. 11. Tritium release by thermal desorption from disks obtained from JET tile 004/2-20 (disk A1 from cylinder 7).

within the accuracy of the measurements, when graphite specimens containing tritium implanted at ion energies between 10 and 50 keV were heated to very high temperatures i.e. $\leqslant$1700 K. This still needs to be confirmed with tiles recovered from a D–T operated machine.

Concerning the detritiation of graphite, the above described release data imply that under these conditions temperatures above 700°C are needed to liberate the tritium from the tiles via heating in a He + 0.1% H_2 purge gas.

3.5. Detritiation of tiles

To get first information on the characteristic temperatures required for the detritiation of a tile, a single plasma exposed A1 disk from cylinder No. 7 of the TFTR tile was cut into three approximately equal segments. By complete combustion at 850°C the tritium concentration in the first segment was found to be 56.4 kBq/g. The second segment was heated in the thermogravimetric balance under a flow of 15 ml/min of synthetic air at a temperature of 400°C for a total of 15 h. The activity remaining in this second segment under these conditions was determined by complete combustion and found to be 2.2 kBq/g. When the experiment was repeated with the third segment at a heating temperature of 450°C the tritium activity remaining in the segment was found to be 0.9 kBq/g. Neither at 400°C nor at 450°C was a measurable weight loss of the respective graphite disk segments observed by thermogravimetry. The fractions of trapped tritium in the disk segments released at 400°C and 450°C were found to be 96.0% and 98.4%, respectively. This high fraction can be explained by a selective combustion of the co-deposited layer under these conditions. Interestingly, there are no indications that at temperatures below 450°C tritium diffuses from the co-deposited layer into the bulk of the material. Generally, these findings are in line with observations from Pacenti et al. [25]. They reported that most of the tritium contained in the co-deposited layer,

i.e. >98%, can be liberated at 600°C in less than 2 h using a nitrogen stream containing 2% hydrogen. Causey et al. [21] showed that for air anneals a temperature of 350°C is sufficient to release all the hydrogen isotopes in the surface layer and attributed this to an isotopic exchange with the water in the air. Thus it appears that it is possible to detritiate graphite tiles at comparatively mild temperatures provided sufficiently long heating periods are selected.

4. Implications of the determined tritium profiles and heat treatments of trititated graphite specimens to the development of a detritiation methodology for graphite tiles

A possible pre-detritiation technique of JET tiles is the mechanical removal of the co-deposited layer. This layer, which is most probably less that 50 μm thick, is – at least in part – comparatively loosely bound. For an effective pre-detritiation, however, not only the thin layer of the plasma-exposed side on the tile must be removed, but also the lateral plasma-exposed layers. To accomplish this quantitatively appears to be complicated. When only the highly contaminated surface layers are removed from the tiles the maximum achievable decontamination factor will be less than 100, i.e. 90, because at least 1.1% of the tritium will remain in the bulk of the tile.

From the results of this work it is apparent that under a helium/hydrogen gas stream tritiated graphite samples need to be heated to temperatures of more than 800°C to release most of the tritium. For the essentially complete tritium liberation from a tile even higher temperatures will be necessary. The detritiation of large tiles under these conditions will thus require rather long baking times at elevated temperatures to achieve the desired high tritium decontamination factors.

When synthetic air is used as sweep gas instead of a noble gas and the graphite tiles are heated for a rather extended period of time, tritium of the order of 98% can be liberated in the range temperature 400–450°C. Under these conditions the degree of graphite combustion is still very small and no significant diffusion of tritium appears to take place from the co-deposited layer into the bulk of the graphite. Further work under more realistic conditions will provide the information needed to decide whether this approach constitutes the most promising to deal with the contaminated tiles.

The complete oxidation of whole tiles to carbon oxides and tritiated water is expected to be technically rather complex. For safety reasons the use of diluted oxygen will be necessary. The thermal oxidation of CFC tiles is expected to be even more difficult than that of graphite tiles, i.e. higher temperatures and longer heating times. In addition, very large gaseous volumes of low level tritium-contaminated carbon oxides will have to be dealt with. The quantitative recovery of small amounts of tritiated water from a large carbon oxide stream will have to be developed.

5. Conclusions

A reliable technique was implemented to determine tritium in graphite based on the complete combustion of graphite specimens with either moist oxygen or moist air followed by the retention of the produced tritiated water in bubblers and quantification of the tritium by liquid scintillation counting. Whereas at temperatures below 800°C an oxide ash remains after combustion of graphite, a complete volatilisation takes place at higher temperatures.

The average concentration of tritium in a TFTR tile exposed to D–D plasmas and in a JET tile exposed to D–T plasmas, corresponding to the integrated effect of numerous discharges and subsequent first wall cleaning steps, was measured to be (6.04 ± 3.23) and (13.8 ± 3.5) kBq/cm^2 of plasma-exposed surface, respectively. The distribution of tritium co-deposited/implanted on the surface of the plasma-exposed side of both tiles was found to be inhomogeneous, the concentrations varying more strongly in the TFTR tile (up to a factor of 11) than in the JET tile (up to a factor of more than 3). More runs presently under way will allow a more general statement concerning this matter.

Many tritium depth profile measurements on reactor graphite tiles have indicated that more than 98.9% of the tritium is co-deposited/implanted on the plasma-exposed side within a surface layer thinner than 50 μm thickness. Tritium is also co-deposited on the graphite in the gaps between the JET tiles. The concentrations, which were found to vary considerably, reached values as high as 5.5 kBq per cm^2 of plasma-exposed surface area.

From the present study it appears that the easiest approach for a first rough decontamination of graphite tiles (DF $\geqslant$ 50) is to heat them up to 400–450°C under a stream of moist air. The released tritium could be converted into tritiated water employing a suitable oxidation catalyst and could be collected downstream either with a bubbler containing water or ethylene glycol, or with an appropriate molecular sieve, e.g. 3A. A tritium migration from the co-deposited layer into the bulk of the graphite was not apparent [26].

The combustion time of graphite is roughly proportional to the sample size and is strongly dependent on both the combustion temperature and the nature of the sample. An expedient full combustion of graphite tiles with moist air is only possible at temperatures exceeding 700°C.

If the highly inhomogeneous tritium surface distribution observed on single tiles has general validity, a tritium inventory determination in a fusion machine based on discreet measurements of the tritium

concentrations on the plasma-exposed side of graphite tiles may lead to errors in global tritium estimates. The considerable fraction of tritium immobilised in the gaps between the tiles also needs to be taken into account. More work on this subject is considered indispensable.

Acknowledgements

The package of work was carried within the frame of contract No JU/13254 with JET, in accordance with the contract technical specifications and appendices [27].

References

[1] P.C. Souers, Hydrogen Properties for Fusion Energy, University of California Press, Berkeley and Los Angeles, California, 1986.
[2] G. Federici, C.H. Wu, B. Esser, Fusion Eng. Design 16 (1991) 393.
[3] H.W. Herrmann, S.J. Zweben, D.S. Darrow, J.R. Timberlake, G.P. Chong, A.A. Haasz, C.S. Pitcher, R.G. Maccaulay-Newcombe, Nuclear Fusion 37 (1997) 293.
[4] R.A. Causey, K.L. Wilson, J. Nucl. Mater. 138 (1986) 57.
[5] M.E. Malinovski, R.A. Causey, J. Vac. Sci. Technol. A 6 (3) (1988) 2130.
[6] R.A. Langley, R.S. Blewer, J. Nucl. Mater. 76&77 (1978) 313.
[7] D.H.J. Goodall, G.M. McCracken, J.P. Coad, R.A. Causey, G. Sadler, O.N. Jarvis, J. Nucl. Mater. 162–164 (1989) 1059.
[8] I. Youle, A.A. Haasz, J. Nucl. Mater. 248 (1997) 64.
[9] J.P. Coad, R. Behrisch, H. Bergsaker, J. Ehrenberg, B. Emmoth, J. Partridge, G. Saibene, R. Sartori, J.C.B. Simpson, W. Wang, J. Nucl. Mater. 162–164 (1989) 533.
[10] P.K. Khabibullaev, B.G. Skorodumov (Eds.), Determination of Hydrogen in Materials, Springer, Berlin, 1989.
[11] G.Y. Sun, M. Friederich, R. Grötzschel, W. Bürger, R. Berhisch, C. Garcia-Rosales, J. Nucl. Mater. 246 (1997) 9.
[12] J. Engelhard, USAEC Report, JUL-752-RG, 1971.
[13] D.E. Vance, M.E. Smith, G.R. Waterbury, LA-7716 UC, 1979.
[14] N.N. Greenwood, A. Earnshaw, Chemistry of the Elements, Pergamon, New York, 1984, p. 303.
[15] Gmelins Handbuch der Chemie, Kohlenstoff, Teil B, System Nr. 14, Verlag Chemie GmbH, Weinheim, 1968, p. 796.
[16] J.W. Mellor, Inorganic and Theoretical Chemistry, Longmans, vol. V, Green and Co., 1955, p. 811.
[17] J.S. Mattson, H.B. Mark Jr., Activated carbon, Marcel Dekker, New York, 1971.
[18] A.T. Peacock, J.P. Coad, K.J. Dietz, A.P. Knight, Tritium retention in first wall material at JET after the first tritium experiment (F.T.E.), Proc. 17th Symp. on Fusion Technol., Rome, Italy, 1992, pp. 329–333.
[19] A.E. Pontau, R.A. Causey, J. Bohdansky, J. Nucl. Mater. 145–147 (1987) 775.
[20] R.A. Causey, J. Nucl. Mater. 162–164 (1989) 151.
[21] R.A. Causey, W.R. Wampler, D. Walsh, J. Nucl. Mater. 176–177 (1990) 987.
[22] K. Masaki, K. Kodama, T. Ando, M. Saidoh, M. Shimuzu, T. Hayashi, K. Okuno, Fusion Eng. Design 31 (1996) 181.
[23] M. Friedrich, G. Sun, R. Grötzschel, R. Behrisch, C. Garcia-Rosales, M.L. Roberts, Nucl. Instrum. and Meth. B 123 (1997) 410.
[24] J.A. Sawicki, J. Roth, L.M. Howe, J. Nucl. Mater. 162–164 (1989) 1019.
[25] P. Pacenti, R.A.H. Edwards, F. Campi, Detritiation of graphite and beryllium plasma-facing components, Proc. 19th Symp. on Fusion Technol., Lisbon, Portugal, 1996, pp. 1705–1708.
[26] R.D. Penzhorn, N. Bekris, P. Coad, L. Dörr, M. Friedrich, M. Glugla, A. Haigh, R. Lässer, A. Peacock, Fusion Eng. and Design, in press.
[27] A. Haigh, Technical Specification for the detritiation of graphite first wall tiles, JU/13254.